Asian Journal of Chemistry; Vol. 31, No. 1 (2019), 61-72

ASIAN JOURNAL OF CHEMISTRY

https://doi.org/10.14233/ajchem.2019.21513

Solvatochromism of Quinoline-390 and Rhodamine-800: Multiple Linear Regression and Computational Approaches

ANIL KUMAR[1], Y.F. NADAF[2] and C.G. RENUKA[3,*]

[1]P.G. Department of Physics, Sri Siddeshwara Govt. First Grade College, Naragund-582207, India
[2]P.G. Department of Physics and Material Research Centre, Maharani Science College for Women, Bengaluru-560001, India
[3]Department of Physics, Jnanabharathi Campus, Bangalore University, Bengaluru-560056, India

*Corresponding author: E-mail: renubub@gmail.com

Received: 13 June 2018; *Accepted*: 1 August 2018; *Published online*: 30 November 2018; AJC-19160

The electronic absorption and emission spectra of laser dyes quinoline-390 and rhodamine-800 in distinct organic solvents have been analyzed to understand conventional interactions of solvents on the intensities, peak positions of both absorption and emission spectrum. The relationship between absorption spectrum (λ_{max}) and solvatochromic constants (ε, n, E) indicates that the peak positions are fundamentally influenced by non-specific and specific kind of interactions between the solute and solvent. Solvent effects on the electronic absorption band shift are characteristics of the degree of charge rearrangement of the solute molecules upon electronic excitation. These spectral shifts reflect the effect of the equilibrium solvents association across the energized solute particle, which adjusts inertially as a result of quick charge realignment upon radiative deactivation to the lowest electronic state. Spectral regression study techniques were carried out for the qualitative chemical analyses of these compounds, which provides an opportunity to assess electrical-optical molecular constants within the excited electronic conditions. Further TD-DFT computational techniques for optimized geometry, electronic structure and Mulliken charge distribution in vacuum and ethanol solvent were carried out to acquire additional knowledge of the molecular arrangement and electronic properties of these laser dyes.

Keywords: Solvatochromism, Quinoline-390, Rhodamine-800, Regression Correlations, TD-DFTQM analysis, Mulliken charges.

INTRODUCTION

The electronic spectra on molecules are normally changed in solvation mechanism. The structure, intensity of either emission or absorption spectra or both endorses alterations when spectrally effective molecules move from gaseous stage to fluid stage. The alterations evoked by a solvent within the electronic spectrum molecules can provide knowledge on the localized electric field acting on spectrally strong molecules [1]. Efforts to prove few experimental relations among the spectral qualities and the perceptible or imperceptible constants of the solution had been theoretically described in a few dynamic and cellular models. Solvatochromism is one amongst the few techniques that let to calculate the localized electric field within the core of liquids, eventually by the strength of the intermolecular interactions. The existing models at the core intermolecular interactions in fluids shows contribution of the few kinds of interactions by using distinct features of solvent parameters, ignoring the existence of probable distinct interactions. Few models solely (in Bakshiev's hypothesis) takes account of extended field interactions, ignoring the availability of specific interactions to the overall shift confined to a prone solvent. Normally, the availability of the specific interactions is articulated *via* semi-empirical terms obsessed on the nearby grouping of the electronic charges within the interacting molecules.

In Bakhshiev hypothesis, the provision of the extended field interactions to the overall spectral shift confined in electronic spectrum of the molecule is articulated by the means of the relation of the form:

$$\tilde{\nu}_{max} = \tilde{\nu}_{max,0} + a_1 F[\varepsilon] + a_2 F[n] \quad (1)$$

In above equation $\tilde{\nu}_{max}$ denotes the maximum absorption wavenumber (cm^{-1}) for a prone solvent, $\tilde{\nu}_{max,0}$ denotes the maximum absorption wavenumber (cm^{-1}) of the similar electronic absorption spectra reported for the gaseous condition

of the solute. $F[\varepsilon] = \frac{\varepsilon - 1}{\varepsilon + 2}$ and $F[n] = \frac{n^2 - 1}{n^2 + 2}$ are solvent functions dependent on dielectric permittivity and index of refraction successively. The secondary and tertiary term in form (eqn. 1) indicate the involvements of the orientation and diffusive triggered-polarization conventional interactions subsequently. One will accept that '$a_1 F[\varepsilon]$' reveal the spectral shift analogy to the directional interactions and '$a_2 F[n]$' is attributed to the diffusive-triggered-directional forces. There is the remarkable quantity of research wherein the distinctive kinds of interactions are proven for various molecular systems.

Specific interactions are normally localized to a region of molecules where atoms have a tendency to form covalent bonds and thus, an articulated neighborhood partition of electric charges gets feasible, or evaluation of few mechanical characteristics of solution once further strategies are utilized. In models like Catalan [2] and Kamlet-Taft [3] solvent polarity scale is explained. Either scales strive to determine the role of solvent-solute interaction by studying the dependency on non-specific and specific interactions. Specific interactions involve hydrogen bond acceptor or/and donor ability while non-specific interactions involve polarity and polarizability interactions [4]. If $\Delta\tilde{\nu}_{sp}$ specific interactions are included in the (eqn. 1) form, one attains of the form:

$$\tilde{\nu}_{max} = \tilde{\nu}_{max,0} + a_1 F[\varepsilon] + a_2 F[n] + \Delta\tilde{\nu}_{sp} \quad (2)$$

where $\Delta\tilde{\nu}_{sp} = a_3\alpha + a_4\beta + a_5\pi^*$. α = hydrogen bond donor, β = hydrogen bond acceptor and π^* = dipolarity/polarizability.

Distinctive kinds of intermolecular interaction in solutions had been confirmed by solvatochromic investigations. The separation of the conventional and specific interactions lets in to calculate the energy of every kind of interactions behaving in solution. Correlations of the form (eqn. 2) or a lot of sophisticated dependents are validated for spectral information, a very important part shows the anomalous information removal, because of the truth that these facts could extensively regulate the esteems of the coefficients of regression a_1 and/or a_2.

Computational procedures are employed to determine the terms which are yielding a predominant influence on the comprehensive spectral shift. The influence of all kind of interaction is accustomed by the goodness of the coefficients of regression, a_i, i = 1, 2, 3, 4. The interactions defined by terms with modest coefficients of regression are eventually over looked.

A decent evaluation of regression coefficients a_1 and/or a_2 provide an opportunity to assess electrical-optical molecular constants within the excited electronic conditions. Greater the statistics of observational information, the more accuracy of the coefficients of regressions decided. The significance of a unique result of the coefficients of regression is because of their usage in an approximation of few electrical-optical constants inclusive of dielectric permittivity or electrical-dipole moment within the molecularly excited conditions [1].

In solvation mechanism, the solvent surroundings decide crucial alterations in optoelectrical characteristics of the spectral energetic molecules in comparison to the ones in its vaporous stage. The reports are presently accessible on the relations of ultraviolet absorption energies with the solvent constants [5-10]. Speculations concerning the solvent activity on electronic spectrum formulated in the recent time [11,12] enable to calculate the optoelectrical parameters, as in polarizability or electric dipole moments for spectrally energetic molecules employing the spectral variations as indications of the potency of the internal interactions. Few macroscopical parameters of the solvent like the index of refraction (n), dielectric permittivity (ε). Whilst microscopic considerations within the lowest electronic conditions are understood by trial or computing, the equivalent esteems in the agitated electronic spectrum could be estimated.

The mechanics of chemical substance reaction will be described on the basis of spectral information in various solvents. The study is a deliberate and thorough investigation of solvent consequences on the electronic spectrum of absorption and emission. It is pointed to explain some application imparting information about the liquid structure, which includes the core forces in fluid stage conjointly permitting on the calculation of the electro-optical constants in the excited conditions [6]. In this regard laser dyes, quinoline-390 (Qu-390) and rhodamine 800 (Rh-800) have been evaluated employing spectrofluorometric derived reviews. No past assurance of this laser dyes has been accounted in works cited.

EXPERIMENTAL

The laser dyes 7-(dimethylamino)-4-methoxy-1-methyl-1,8-naphthyridine-2(1*H*)-one (quinoline-390) and 9-cyano-2,3,6,7,12,13,16,17-octahyro-1*H*,5*H*,11*H*,15*H*-xantheno-[2,3,4-ij:5,6,7-i′j′]diquinolizin-4-ium perchlorate (rhodamine-800) are purchased from Exciton Company USA, has been used without further purification. Optimized structures of Qu-390 and Rh-800 are shown in Figs. 1 and 2. In the current study, the solvents used are namely acetone, acetonitrile, butanol, cyclohexane, dioxane, DMSO, ethanol, ethyl acetate, hexadecane, hexane, methanol, pentadecane, propanol, toluene and water are commercially available S.D. Fine Chemicals Ltd., India and all are of spectroscopic grade, used without further purification.

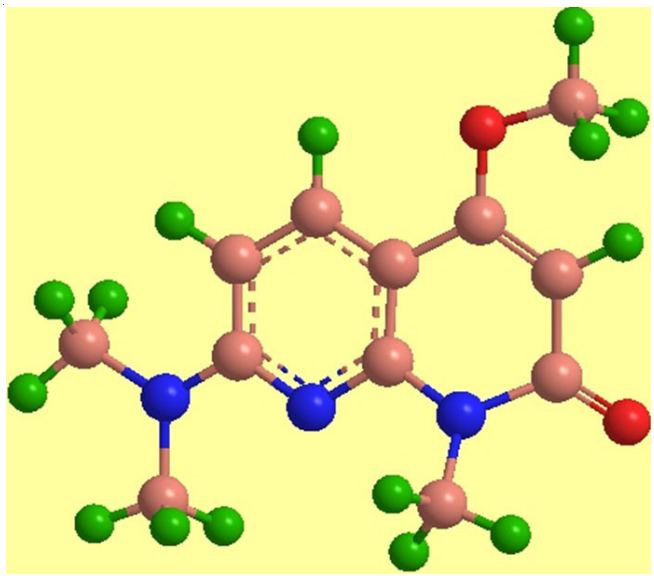

Fig. 1. Optimized molecular structure of quinoline-390

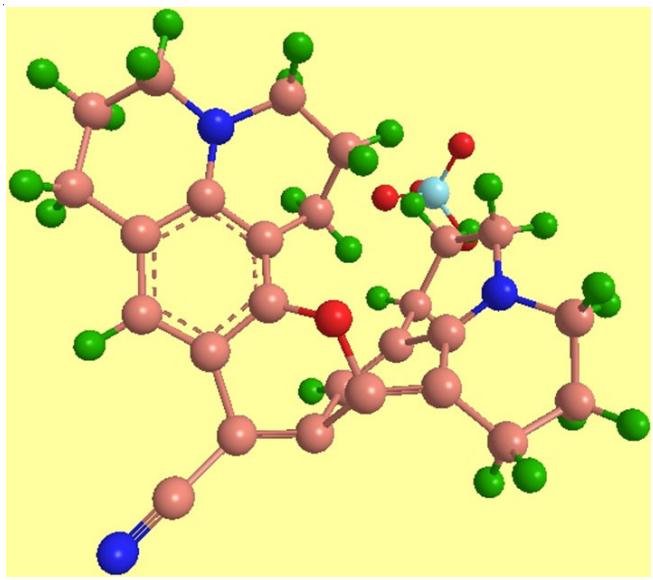

Fig. 2. Optimized molecular structure of rhodamine-800

Experimental techniques: The UV-visible absorption studies were carried out on a Shimadzu UV-1800 spectrometer. steady-state fluorescence studies were carried out on Hitachi F-2700 Fluorescence Spectrophotometer. All the measurements were performed at 25 °C temperature with solutions concentration range 10^{-5}-10^{-6} mol dm^{-3}. The solvent parameters are obtained from the literature [13].

Theoretical context:

Specific interactions and solvents effects among solvent and solute particles are main constituents in elucidating their behaviour of spectra [14,15]. For regression studies the subsequent form has been utilized:

$$G = a_0 + a_1H_1 + a_2H_2 + a_3H_3 + a_4H_4 + ... \quad (3)$$

where a_1, a_2, a_3 and a_4 are distinct coefficients of regression and a_0 is the invariable regression intercept. The ascertained peak region $\lambda_{maximum}$ is considered as dependent variable G, at the same time the independent variables (H_1, H_2, H_3, H_4….) are the ones for solvents interaction processes, (ε, n, E) or (E, P, Q, R) Tables 1 and 2. The quantity 'n' is the index of refraction, 'ε' is the electric dielectric permittivity, E is an experimental polarity of solvent susceptible to each solute-solvent dipolar and hydrogen coupling interactions [16,17]. The measure P relies on ε, which is a measure of the solvent polarity agent, $P = \frac{[\varepsilon - 1]}{[2\varepsilon + 1]}$. The measure Q relies on the

TABLE-1
SOLVATOCHROMIC PARAMETERS USED IN THE CORRELATION STUDIES

Solvent	n	ε	E	P	Q	R
Hexane	1.480	1.89	31.0	0.186	0.221	-0.055
Cyclohexane	1.426	2.02	30.9	0.202	0.204	-0.002
Pentadecane	1.431	2.039	–	0.205	0.206	-0.002
Hexadecane	1.434	2.046	–	0.205	0.207	-0.002
Dioxane	1.420	2.210	36.0	0.223	0.202	0.034
Toluene	1.497	2.379	33.9	0.239	0.226	0.022
Ethylacetate	1.370	6.020	38.1	0.385	0.184	0.400
Butanol	1.400	17.51	49.7	0.458	0.195	0.604
Propanol	1.380	20.45	50.7	0.464	0.188	0.635
Acetone	1.360	20.56	42.2	0.464	0.181	0.646
Ethanol	1.360	24.55	51.9	0.470	0.181	0.666
Methanol	1.330	32.66	55.4	0.477	0.169	0.709
Acetonitrile	1.340	35.94	45.6	0.479	0.173	0.711
Dimethyl sulfoxide	1.480	46.45	45.1	0.484	0.221	0.654
Water	1.330	78.50	63.1	0.491	0.169	0.759

TABLE-2
SPECTRAL DATA FOR Qu-390 AND Rh-800 SAMPLES IN DIFFERENT SOLVENTS MEDIA

Solvents	Qu-390			Rh-800		
	λ_{max}^{abs} (nm)	λ_{max}^{ems} (nm)	$\Delta\tilde{\nu}$ (cm^{-1})	λ_{max}^{abs} (nm)	λ_{max}^{ems} (nm)	$\Delta\tilde{\nu}$ (cm^{-1})
Cyclohexane	359.09	374.99	1181.14	–	–	–
Pentadecane	355.47	376.07	1541.18	–	–	–
Hexadecane	353.09	375.79	1711.42	–	–	–
Dioxane	357.08	381.23	1774.04	256.8	437.93	16106.1
Toluene	350.87	381.41	2282.14	–	–	–
Ethyl acetate	348.37	380.88	2450.19	271.8	440.23	14076.3
Butanol	346.90	382.93	2712.31	272.6	455.63	14736.1
Propanol	346.28	384.37	2861.76	270.1	470.97	15790.5
Acetone	352.01	389.98	2766.75	257.8	418.16	14875.4
Ethanol	355.90	382.76	1971.88	263.8	–	–
Methanol	355.98	383.42	2010.40	269.7	462.51	15457.1
Acetonitrile	355.85	382.61	1965.97	268.5	455.38	15284.2
Hexane	356.92	374.46	1312.36	271.3	460.53	15145.4
Dimethyl sulfoxide	357.31	387.31	2167.79	256.3	–	–
Water	356.21	385.48	2131.64	268.7	–	–

TABLE-3
MULTIPLE LINEAR REGRESSION CORRELATION COEFFICIENTS (MCC) FOR SAMPLES USING DIELECTRIC PERMITTIVITY (ε), INDEX OF REFRACTION (n), EXPERIMENTAL POLARITY (E) AND THEIR COMBINATIONS SOLVENT PARAMETERS FOR λ_{max}(abs)

Parameters	Qu-390				Rh-800			
	a_1	a_2	a_3	MCC	a_1	a_2	a_3	MCC
ε	-1.66895			0.3730	2.67522			0.4945
N	-617.666			0.3440	-1157.13			0.5335
E	-0.10384			0.0188	4.97117			0.7443
ε, n	-2.36103	-907.298		0.6090	1.97762	-914.535		0.6369
ε, E	-2.58613	1.85046		0.4575	0.33783	4.71587		0.7459
n, E	-890.449	-1.57031		0.4198	-411.219	4.29394		0.7613
ε, n, E	-2.51257	-860.179	0.37826	0.6109	0.37337	-415.717	4.00437	0.7633

TABLE-4
MULTIPLE LINEAR REGRESSION CORRELATION COEFFICIENTS (MCC) FOR SAMPLES USING E, P, Q AND RAND THEIR COMBINATIONS SOLVENT PARAMETERS FOR λ_{max}(abs)

Parameters	Qu-390					Rh-800				
	a_1	a_2	a_3	a_4	MCC	a_1	a_2	a_3	a_4	MCC
E	-0.104				0.0188	-0.104				0.7443
P	-177.7				0.2228	790.2				0.8196
Q	-1764.				0.3371	-521.1				0.5499
R	-63.71				0.2038	43.85				0.7750
E, P	2.058	-406.1			0.3263	1.865	583.21			0.8389
E, Q	-1.617	-2607			0.4163	4.295	-1163.5			0.7600
E, R	1.926	-148.2			0.3001	1.898	224.31			0.8335
P, Q	-401.4	-3038			0.5548	704.19	-1167			0.8354
P, R	-1721	607.7			0.2908	991.70	-79.356			0.8199
Q, R	-3345	-172.8			0.5728	-839.0	280.18			0.8214
E, P, Q	0.735	-471	-2876		0.5606	1.478	564.21	-841.6		0.8461
E, P, R	1.845	-1639	494.9		0.3592	1.951	1077.8	-198.5		0.8403
E, Q, R	0.855	-3199	-205.5		0.5806	1.715	-545.73	214.52		0.8364
P, Q, R	3654	-5407	-1666		0.6429	4158.6	-3185	-1419		0.8662
E, P, Q, R	0.327	3561.1	-5298	-1640.	0.6439	1.1476	3829.64	-2803	-1328	0.8723

refractive index (n) of solvent which is a measure of solvent evoked dipole-solute permanent dipole interactions, Q = $\frac{[n^2-1]}{[2n^2+1]}$, though R is a measure of permanent dipole-permanent dipole interactions, $R = \left(\frac{(\varepsilon-1)}{(2\varepsilon+1)} - \frac{(n^2-1)}{(n^2+2)}\right)$.

Multiple regression analysis techniques was executed for every situation using Origin 8.5 software. The fits are procured as an element of 1, 2, 3 or 4 of this constant [18-21]. The findings are recorded in Tables 3 and 4. The regression coefficients C_1, C_2 and ν_0 (vaporous) have been evaluated employing multiple correlation regression approaches based on the subsequent form:

$$\nu[\text{Solution}] = \nu_0[\text{vaporous}] + C_1\left(\frac{(2\varepsilon-2}{(2\varepsilon+1)}\right) + C_2\left(\frac{(2n^2-2}{(2n^2+1)}\right) \quad (4)$$

where ν_0[vaporous] denotes the energy of spectral maxima in the absenteeism of solvents. Coefficients of multiple relations, statistical measures (R^2) of the coefficient correlations for every R^2 (ν, ε) and R^2 (ν, n^2) compositions have been evaluated and the findings are tabulated in Table-5.

TABLE-5
MULTIPLE LINEAR REGRESSION ANALYSIS DATA FOR SAMPLES Qu-390 AND Rh-800

Sample	Intercept ν_0	C_1	C_2	MCC
Qu 390	1026.02	-200.693	-1518.9	0.5548
Rh 800	148.125	352.099	-583.809	0.8354

RESULTS AND DISCUSSION

Solvatochromic absorption–multiple regression relations analysis: The shifting in spectra of these samples in solvents of various polarities are effects of contrasts in solvation of difference among the excited and ground state conditions. Those shifts inside the spectral locations speculate the influences of solvent ability on the solvation energy of dissolving agent that which sequentially relies upon the activity of non-specific and specific intermolecular interactions within solvent and solute particles agreeable to Reichardt [15]. Multi-parameter analysis of solvents influence had been considered for an exhaustive explanation of the solute λ_{max}^{abs} spectral variations. In comparison the relationship of λ_{max} for laser dyes Qu-390 and Rh-800 with the dissolving agent parameter, an impression has arrived approximately regarding the sort of interactions among the solvent and solute. The solvatochromic shifts affirm the effect of the index of refraction and dielectric constant of the solvents and in addition solvent-solute hydrogen interactions [22].

Numerous one, two, three and four constants forms were accustomed to relate the spectral shifts with distinct experimental solvent polarity employing the multiple linear coefficient regressions methods. Tables 3 and 4 are examples, typical

displaying the effects of regression studies of energy transits of laser dyes. Multiple correlation coefficients (MCC) have been employed to achieve the consistency of essentials to the parameter. The values of MCC has been considered as a degree of excellence to the fitting if MCC values are high (almost one) [23]. This implies that a specific dissolving agent constant has a great relationship to the spectral shift. If MCC is low (almost zero) implies a poor relation to the spectral shift. The evaluation of the spectral shifts of the energy transits of Qu-390 and Rh-800 using one and more constants are recorded in Tables 3 and 4.

One constant relation among λ^{abs}_{max} Qu-390 and Rh-800 with ε, n or E reveals a high dependence of dielectric permittivity, index of refraction and solvent polarity for Rh-800 than Qu-390. The relations of solvent polarity for Rh-800 and Qu-390 are 0.7443 and 0.0188 individually, this suggests the solvatochromic role for the transits in Rh-800 is specially governed through the solvent ability to create the hydrogen-coupling with the solute particles besides the electric dipole interactions [24]. The value of MCC 0.0188 for Qu-390 could be elucidated in terms of solute permanent electric dipole-solvent permanent electric dipole interactions. The relations for Qu-390 isn't that acceptable great and this indicates one parameter can't manipulate the spectral modifications, thus the combos are needed. The alternation correlations of the two-parameter forms with solvent spectral shift were conjointly contemplated and gave obviously as anticipated higher fitting to that spectral shift than relating one parameter fitting for each sample. Correlations with two solvent constants for Qu-390, (ε, n) and (ε, E) with MCC = 0.6090 and 0.4575 respectively shows the better influence of those constants on the position maxima wavelength than (n, E) with MCC = 0.4198 [25].

For the Qu-390 development of the fittings took place once employing three constants [ε, n, E] respectively better coefficient of correlation have been attained therein case (MCC = 0.6109) suggests that dielectric consistent play a task in the determined spectral shift. Further influence of index of refraction on the spectral shift of λ^{abs}_{max} is truly seen in Qu-390. However, the MCC values determined while employing other constant E is 0.0188 implies that there has been no importance of this constant on the spectral shift for Qu-390. The relations for Rh-800 had a slight gain of fitting had proved when employing two or three constants (ε, n), (ε, E) (n, E) (ε, n, E) in such case of chemical substance indicating their effects in a different procedure. However, the MCC values accomplished when employing different constants E is 0.7443 intimates that hydrogen coupling plays an important task in spectral shift together with refractive index and dielectric permittivity.

Relations amongst λ^{abs}_{max} of Qu-390 and Rh-800 with each solvatochromic parameter E, P, Q and R in Table-4 exhibits dependency of λ^{abs}_{max} of laser dyes. A, one constant relation among λ^{abs}_{max} for Qu-390 and Rh-800 with either E, P, Q or R reveals a high dependency of dielectric constant, index of refraction and solvent polarity for Rh-800 than Qu-390. The correlations of constants P for Rh-800 and Qu-390 are 0.8196 and 0.2228 respectively, this indicates the solvatochromic activity for the transits in Rh-800 is generally inhibited *via* solvent polarity. Nonetheless with parameters E (0.7443), Q (0.5499) and R (0.7550) in case of Rh-800 does effects the solvatochromism. The MCC values (0.0188, 0.2228, 0.3371 and 0.2038) for Qu-390 could be elucidated in particulars of solute permanent electric dipole-solvent electric dipole interactions. The correlations of the two constant forms with dissolving agent spectral shift were additionally contemplated and obviously gave as anticipated good fittings to those spectral shifts than the relating one parameter fitting for each dye [26]. Correlations with two constants for Qu-390 (P, Q) and (Q, R) with MCC values of 0.5548 and 0.5728, respectively suggests the greater influences of solvent polarity, a measure of solute permanent electric dipole-solvent evoked electric dipole interaction and permanent electric dipole-permanent electric dipole interaction on particular λ^{abs}_{max} positions than (E, P), (E, Q), (E, R) and (P, R).

For Qu-390 betterment of fittings took place while using triad and tetrad constants [(E, P, Q), (E, Q, R), (P, Q, R), (E, P, Q, R)] with MCC values 0.5606, 0.5806, 0.6429 and 0.6439, respectively. Therefore, greater coefficient of relations had been achieved in event (MCC = 0.6439) suggests (E, P, Q, R) play a notable act on shifts. Nonetheless the constant Q (MCC = 0.3371) suggests that Q plays a notable act alongside E P and R. The relationships for Rh-800 had slight gain of fitting was proved while employing two, three and four constants in event of chemical substance Rh-800 suggesting their effect in distinctive mode. Although the values of MCC gained while employing other constant P is 0.8196, suggests that the solvent polarity plays a substantial role in spectral shift, in addition to experimental solvent polarity and permanent electric dipole-permanent electric dipole interaction. As a consequence, for Qu-390 on studying solvent permanent dipole-solute permanent dipole interaction accumulated with the dipolar interactions, addition to solvent refractive index and electrical permittivity is rendering primarily to the empiric solvatochromism. For Rh-800 solute permanent dipole-solvent permanent dipole interactions accumulated with solvent H-bonding ability and/or dipolar interactions and index of refraction is rendering primarily to the empiric solvatochromism. The estimations of C_1, C_2 and ν_0 (vaporous), $R^2(\tilde{\nu}, \varepsilon)$ and $R^2(\tilde{\nu}, n^2)$ and regressions MCC for these laser dyes have been calculated and recorded in Table-5. The statistics suggests that each refractive of index and electric permittivity of the solvents influence the electronic absorption spectra of laser dyes solely to varied energy levels. The poor estimated values of C_1 and C_2 implies the prevalence of robust solvent-solute interactions that motive a lower in strength for the electric transits from lowest occupied molecular orbitals to highest occupied orbitals in compare with the vaporous state. Typically, it can be concluded that the accession of third solvent constant to two constant forms invariably upthrust enhancements within the correlations with the solvent agent evoked spectral shifts. In many events, the distinct three constants combining, suggests that specific solvent-solute interaction especially H-coupling and non-specific solvent-solute interactions inclusive of dispersive and dipolar consequences had furnished an affordable version for explaining the solvent triggered spectral shifts in a prophetic way [27].

Electronic absorption spectrum: The absorption and fluorescence spectrum of individual laser dyes have been

inscribed in a varied solvents of various physical characteristics, predominantly dielectric consistent (ε) and index of refraction (n). Typically, the influence of solvents upon absorption spectrum on these compounds comprises of dislodging and does no longer include a basic difference of standard shape trends of the spectrum. The absorption and emission of these compounds are irritated by varied solvents and therefore the spectral shifts are totally different for the absorption spectra from the ones of fluorescence spectra. The UV-visible absorption spectra for compounds Qu-390 and Rh-800 were recorded at 25 °C in distinct non-polar and polar solvents with distinctive polarities. Preferred data are compiled in Table-2. A λ^{abs}_{max} and solvent constants demonstrate that no cleared red shifts either in the emission nor absorption maxima with the increment of relevant electric permittivity of the solvent [28].

The electronic absorption spectra for Qu-390 and Rh-800 are shown in Fig. 3 and 5, respectively in various solvents. It's evident that the structure of a molecule of the laser dye samples and the polarity of the intermediate each are of immense significance to have an influence on the spectral behaviour of laser dyes. The highest λ^{abs}_{max} 357.31 nm and lowest λ^{abs}_{max} is 346.28 nm for Qu-390, these bands imply that distinctive electronic transits are included. The primary one within the wavelength domain 250-300 nm in Qu-390 could be attributed to the action of π electronic negative charges of the aromatic structure, those bands are delicate to the substitute at the aromatic rings and its slight effect by altering the solvent polarity affirming π-π* attributes of the electronic transits. The secondary one within the wavelength domain 346-360 nm could be attributed excitation of a lone pair of electrical negative charges n-π* which relies upon the polarity of the solvent. In the wavelength domain, 346-360 nm double peaks are seen with minor change are probably attributed to the interaction amongst permanent electric dipole-permanent electric dipole interactions of the solvent with the solute prompted interactions that rely upon n and ε [29]. For Rh-800 the electronic absorption (Fig. 5) in distinct solvent exhibits a feeble and broad spectrum in the domain 250-300 nm as a result of π-π* transits. This shift is essential because of solvent-solute interactions such as H-bonding and dipolar interactions that account steadiness of π* orbitals greater than the π-orbitals. The widespread character of few groups is apparently because of blending of the lowest electronic condition of the hydrogen reinforced complex with distinct electronic states, due to charge exchange from the electron donor particle.

Solvent influences on fluorescence spectrum: The solvent influences on spectral peak positions and their maximum value of the visible light bands of both laser dyes Qu-390 and Rh-800 are recorded in Table-2. From the Figs. 4 and 6 show an emission at λ_{max} is 356.21 nm in water for Qu-390 and λ_{max} is 470.97nm in propanol for Rh-800 due to π-π* and n-π* transitions, respectively. In Rh-800 shows there is no fluorescence information in cyclohexane, DMSO, ethanol, hexadecane, pentadecane, toluene and water, since the least excited state is n-π* conditions prefers non-radiative inter-system traversing as a method of inactivation of the lower most excited singlet state. The rise of a tiny quantity of acid ends up in H-bonding with unpaired bonds elevating the strength of n-π* state to any amount that the least excited condition π-π* turns into least energized condition making fluorescence to occur [30,31].

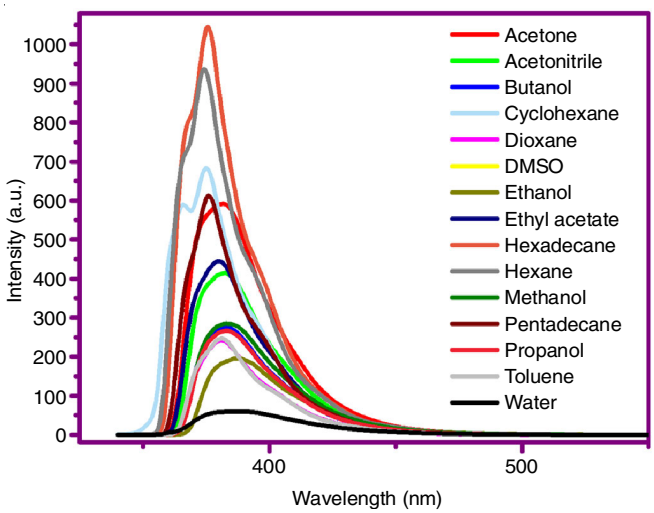

Fig. 4. Fluorescence spectra for quinoline-390 in all studied solvents

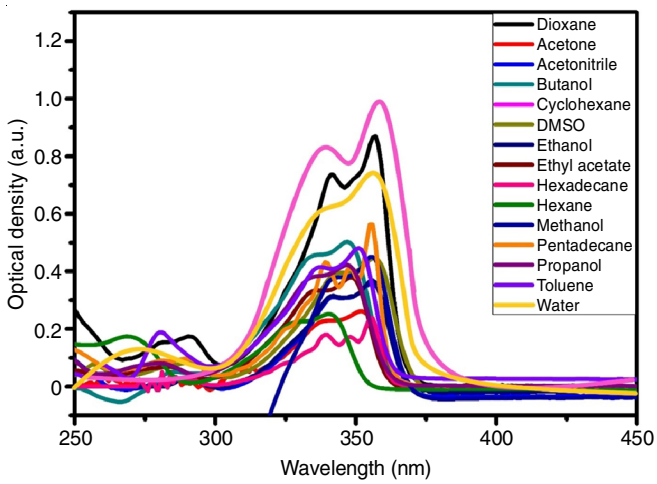

Fig. 3. UV-visible spectrum for quinoline-390 in all studied solvents

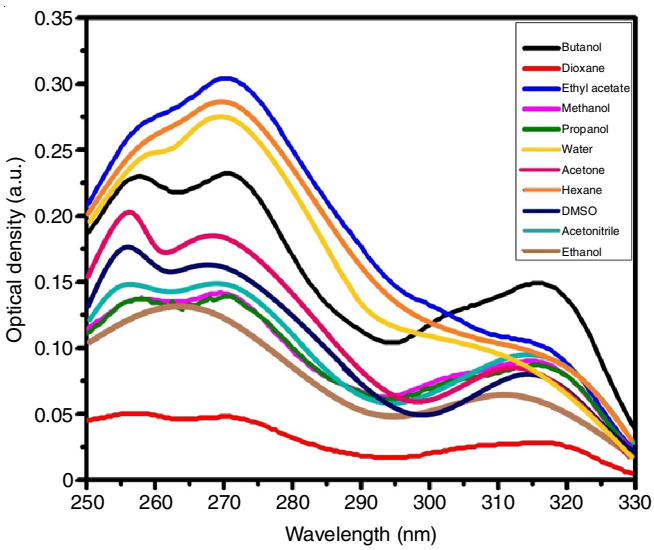

Fig. 5. UV-visible spectrum for rhodamine-800 in all studied solvents

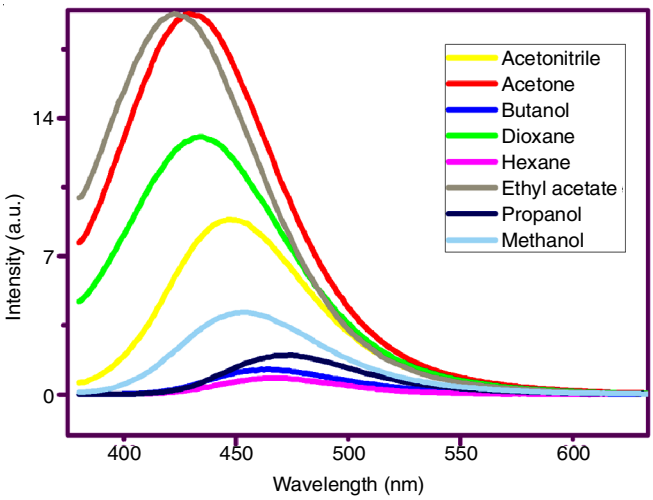

Fig. 6. Fluorescence spectra for rhodamine-800 in all studied solvents

Computational techniques for optimized geometry, electronic structure, Mullikan charge distribution and molecular electrostatic potential: To acquire additional knowledge of the molecular arrangement and electronic properties for quinoline-390 and rhodamine-800, we studied theoretical TD-DFT quantum mechanical computations, which were executed in GAMESS [32]. For molecular optimization, single point energy, molecular orbitals (HUMO, LUMO) and Mullikan charge distributions were theoretical calculated in vacuum and ethanol with 6-31G basis set. The absorption energy's, orbital contributions and oscillator energy towards the minimum ten levels of singlet-singlet transits in the optimized geometry of the ground condition were acquired through computations employing the identical basis set in regard to optimized geometry.

Molecular orbitals study: The molecular orbital plays a vital role in electro-optical properties, in addition, chemical reaction and UV-visible spectrum. The most prominent molecular orbitals are highest occupied molecular orbital (HOMO) and the lowest unoccupied molecular orbital (LUMO). HOMO indicates the variously distinguished donor orbitals, renders the capability to donate an electron and LUMO suggests that of prominent acceptor orbitals, explain the capability to obtain electron. HOMO-2, HOMO-1, LUMO+1 and LUMO+2 renders different donor and acceptors levels, such orbitals specify the way molecule interacts with different species [33-35]. Molecular orbitals calculated in vacuum and ethanol media were used to elucidate information regarding the transferring of charges within the molecule. Molecular orbitals for HOMO-2, HOMO-1, HOMO, LUMO, LUMO+1 and LUMO+2 for Qu-390 and Rh-800 are pictured in Fig. 7. Tables 6 and 8 reveals the HOMO-LUMO energy details for Qu-390, Rh-800 in vacuum and ethanol media.

For HOMO, Qu-390 for the electrons in a vacuum are localized [36-39] on (N13, N1) nitrogen atoms, (C2, C3, C5, C6, C9) carbon atoms and (O11) oxygen atom. In ethanol electrons are localized on (N13, N1) nitrogen atoms, (C2, C3, C4, C5, C6, C8, C9) carbon atoms, (H26) hydrogen atom and (O11) oxygen atom. For Rh-800 in a vacuum, electrons are localized on (N5, N15) nitrogen atoms and (C9, C10, C1, C22, C28, C19, C20, C11) carbon atoms. In ethanol, the electronis localized least localized on (N5) than (N30, N15) nitrogen atoms, (C26, C27, C28 are most localized) than (C10, C23, C24, C25, C21, C11, C20, C26, C27, C28) carbon atoms. For LUMO Qu-390 the electrons in a vacuum are localized on (N13, N1 and N7) nitrogen atoms, (C2, C4, C6, C5, C10, C9, C8) carbon atoms, (011, 016) oxygen atoms [40,41]. In ethanol, electrons are also localized on all atoms as in vacuum except (C6) carbon atom and (N1) nitrogen atom. For Rh-800 the electrons in a vacuum are localized on (N5, N15, N30) nitrogen atoms, (C9, C10, C23, C22, C24, C21, C26, C28, C27, C11, C20) carbon atoms and (O25, O30) oxygen atom. In ethanol, electrons are also localized on all atoms as in vacuum except (C9, C22) carbon atoms, (O35) oxygen atom and (C11, C20, C26, C27, C28) carbon atoms are more localized in ethanol than vacuum [42].

For solute Qu-390 in a vacuum we observed that there is no considerable change in positions of HOMO, HOMO-2 except delocalization on (C10, C9) carbon atoms in HOMO-1. In ethanol, media HOMO-2 are mostly localized on (C3, C4, C6, C10, C9) carbon atoms. In the LUMO+1 (except C9 and C10 carbon atoms in a vacuum) and LUMO+2 orbitals of Qu-390 are localized same as in LUMO in both vacuum and ethanol [43]. The laser dyes Rh-800 in a vacuum there is no significant change in positions of HOMO-1, HOMO-2 than HOMO. In ethanol media, Rh-800 electrons are localized only on (C9, C21, C22, C23) carbon atoms in HOMO-1. There is the localization of electrons only on perchlorate group both in ethanol and vacuums for Rh-800 LUMO's orbitals [44].

From the molecular orbitals studies, HOMO energy (E_{HOMO}) and LUMO energy (E_{LUMO}), energy values for E_{HOMO} and E_{LUMO} of Qu-90 in vacuum found to be -0.2881 eV and -0.0191 eV respectively. Rh-800 same energies found to be -0.2897 eV and -0.0997 eV. The HOMO and LUMO energy band gap found to be 0.2690 eV and 0.1900 eV for Qu-390 and Rh-800 subsequently in vacuum [45]. Other molecular orbital states energies for Qu-390 and Rh-800 in different media are listed in Tables 6 and 7. It is observed from the

TABLE-6
HOMO AND LUMO ENERGY DETAILS FOR Qu-390 IN VACUUM AND ETHANOL MEDIA

Orbital	Energy (eV)		Orbital states	Oscillator strength		Dipole in Debye	
	Vacuum	Ethanol		Vacuum	Ethanol	Vacuum	Ethanol
H-2	-0.3491	-0.2783	H → L	0.8960	0.6549	7.5603	26.1074
H-1	-0.3426	-0.2665	H-2 → L	0.1055	0.4773	9.8583	17.7885
H	-0.2881	-0.2029	H-1 → L	0.4265	0.0439	5.9028	24.2885
L	-0.0191	0.0378	H → L+1	0.2245	0.3067	5.2769	24.3181
L+1	0.10136	0.0824	H → L+2	0.2651	0.2833	8.4392	16.4882
L+2	0.02731	0.0985	H-2 → L+1	0.0300	0.1925	6.1678	16.6487

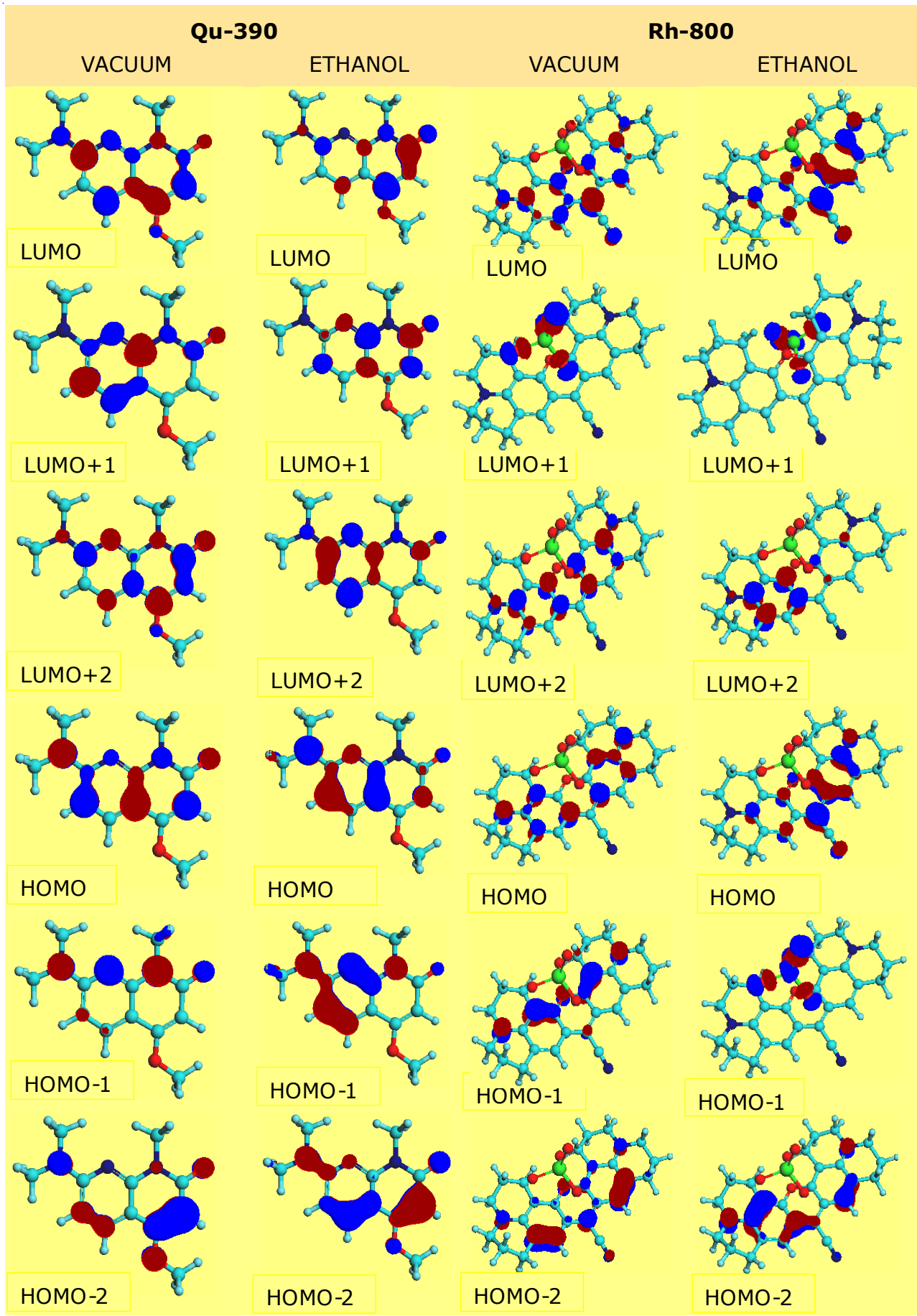

Fig. 7. Plots of frontier molecular orbitals for Qu-390, Rh-800 in vacuum and ethanol

TABLE-7
HOMO AND LUMO ENERGY DETAILS FOR Rh-800 IN VACUUM AND ETHANOL MEDIA

Orbital	Energy (eV)		Orbital states	Oscillator strength		Dipole in Debye	
	Vacuum	Ethanol		Vacuum	Ethanol	Vacuum	Ethanol
H-2	-0.3461	-0.3342	H → L	1.3103	1.5993	13.7629	28.2609
H-1	-0.3212	-0.3062	H-2→ L	0.5223	0.1615	12.6097	19.0001
H	-0.2897	-0.2675	H-1→ L	0.0030	0.0501	15.2825	28.1278
L	-0.0997	-0.0849	H → L+1	0.3453	0.0015	12.8802	45.5542
L+1	-0.0129	-0.0351	H → L+2	0.1299	0.3254	14.4497	39.4566
L+2	0.0050	-0.0111	H-2→ L+1	0.0154	0.0006	12.6409	37.8204

Tables 6 and 7 of Qu-390 and Rh-800 small energy values of HOMO-LUMO, a molecule with small orbital energy gap is known as excitation energy which implies π-π* transitions is easier, high chemical reactivity of molecule towards electron transfer and newly employed to establish the bioactivity from ICT (intramolecular charge transfer) [46-48] together low kinetic stability. Using molecular orbitals energies, Global chemical reactivity configurations of laser dyes such as electronegativity [χ], chemical potential [μ], softness [S], hardness [η] and electrophilicity [ω] configurations are calculated in both vacuum and ethanol using the following equations and results are tabulated in Table-8.

$$\chi = \left(\frac{E_{HOMO} + E_{LUMO}}{2} \right) \quad (5)$$

$$\mu = -\chi \quad (6)$$

$$\eta = \left(\frac{E_{HOMO} - E_{LUMO}}{2} \right) \quad (7)$$

$$\omega = \left(\frac{[(E_{LUMO} + E_{HOMO})/2]^2}{2\eta} \right) \quad (8)$$

$$S = \frac{1}{2\eta} \quad (9)$$

where E_{HOMO} – HOMO energy was correlated to ionization potential, E_{LUMO} – LUMO energy was correlated to electron affinity. From Table-8, the energy gap for Rh-800 is less than Qu-390 hence Rh-800 can be considered as high reactive and soft than Qu-390.

TABLE-8
PHYSICO-CHEMICAL PROPERTIES FOR Qu-390 AND Rh-800

Parameters (eV)	Qu-390		Rh-800	
	Vacuum	Ethanol	Vacuum	Ethanol
HOMO energy	-0.2881	-0.2029	-0.2897	-0.2676
LUMO energy	-0.0191	0.0378	-0.0997	-0.0849
Energy gap	0.2690	0.2407	0.1900	0.1827
Electronegativity	-0.1536	-0.0826	-0.1947	-0.1763
Chemical potential	0.1536	0.0826	0.1947	0.1763
Global hardness	-0.1345	-0.1204	-0.0950	-0.0914
Electrophilicity	-0.08771	-0.0283	-0.1995	-0.1700
Global softness	-0.06725	-0.0602	-0.0475	-0.0457

Opto-electronic parameters could be determined *via* spectral method when molecule and solute are energetic to both electronic fluorescence and absorption. Molecular orbitals infer the transfers of charges within the molecules results in a change in dipole moments and oscillator strength. Dipole moments and oscillator strength are tabulated in Tables 6 and 8.

It also infers from Tables 6 and 7, there is a minor change in the values of dipole moments within the vacuum and ethanol in all transitions between energy levels for both Qu-390 and Rh-800. The values of oscillator strength amongst H→L, higher in a vacuum and comparatively lower values in ethanol media for Qu-390 and the opposite trend follows in Rh-800.

Molecular electrostatic potential (MEP): Computed plots of MEP for Qu-390 and Rh-800 in both vacuum and ethanol solvent is shown in Figs. 8 and 9 which is according to electron density on various points of the molecule, helps in gaining the location of nucleophilic reactions, electrophilic strikes in addition to hydrogen bonding interactions within solvents. Diverse value of electrostatic potential in the surface is exhibited with dissimilar colours [49,50]. The negative (red) area, positive (blue) area of MEP been associated with electrophilic reactivity, nucleophilic reactivity and neutral (green) area.

For Qu-390 contour values of MEP are in the range from -0.0409-0.0409, -0.0491-0.0491 for both in vacuum and ethanol respectively. In vacuum and ethanol electrophilic reactivity are predominantly localized on O-11 oxygen atom, nucleophilic reactivity on methyl groups attached to N-13 nitrogen atom, O-16 oxygen atom and neutral region over pyridine, 1-methyl-2-oxopiperidin-4-olate group except nucleophilic reactivity on pyridine group in ethanol. For Rh-800 contour values for both in vacuum and ethanol ranges from -0.0409-0.0409 and -0.1636-0.1636, respectively [51-53]. In vacuum electrophilic reactivity are predominantly localized on oxygen atoms of perchlorate group, nucleophilic reactivity localized almost over entire region of compound. In ethanol electrophilic reactivity are predominantly localized on oxygen atoms of perchlorate group, nucleophilic reactivity is partly localized on 2,3,6,7-tetrahyro-1*H*,5*H*-pyrido[3,2,1-ij] quinoline group. Neutral region over 9-methyl-2,3,6,7,10,11-hexahydro-1*H*,5*H*-pyrano[2,3-f] pyrido [3,2,1-ij] quinolin-4-ium group [54-56].

Mullikan atomic charge distribution studies: The atomic charge dissemination of the organic molecules characterizes the charges of each and every atom within the molecule. Additionally, the charge dissemination on the organic molecules has a vital effect on vibrational spectrum. Dissemination of negative and positive charges is vital to enlarging or shortening of atomic size and atomic bond length amongst the atoms. The literature survey exhibits that tremendous atomic calculations gave a vital function in the utilization of chemical esti-

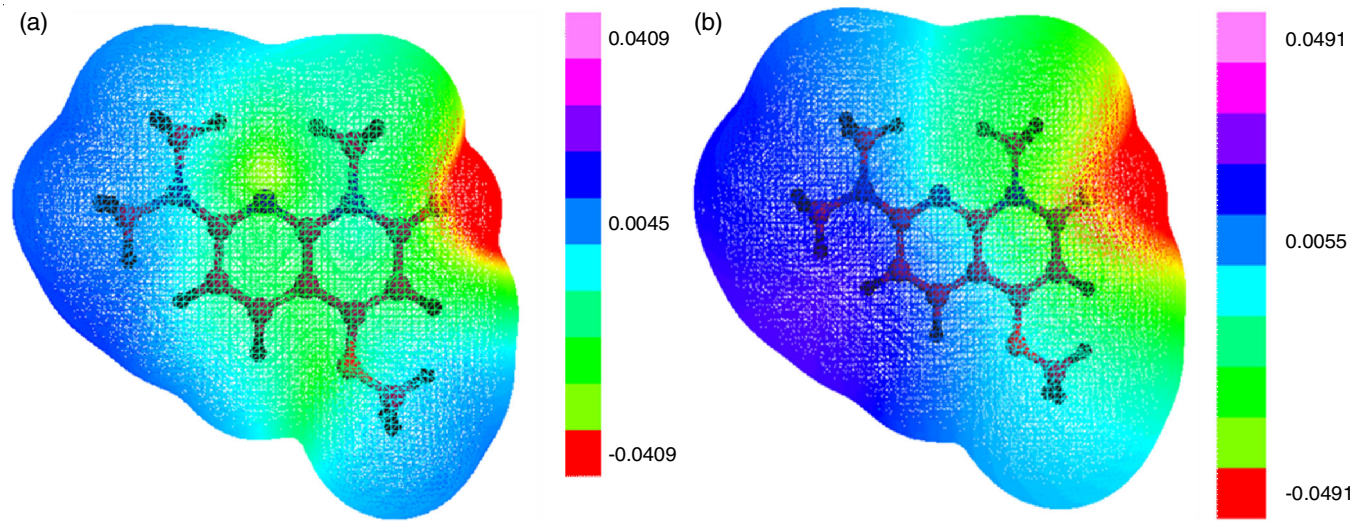

Fig. 8. MEP for Qu-390 (a) in vacuum (b)in ethanol

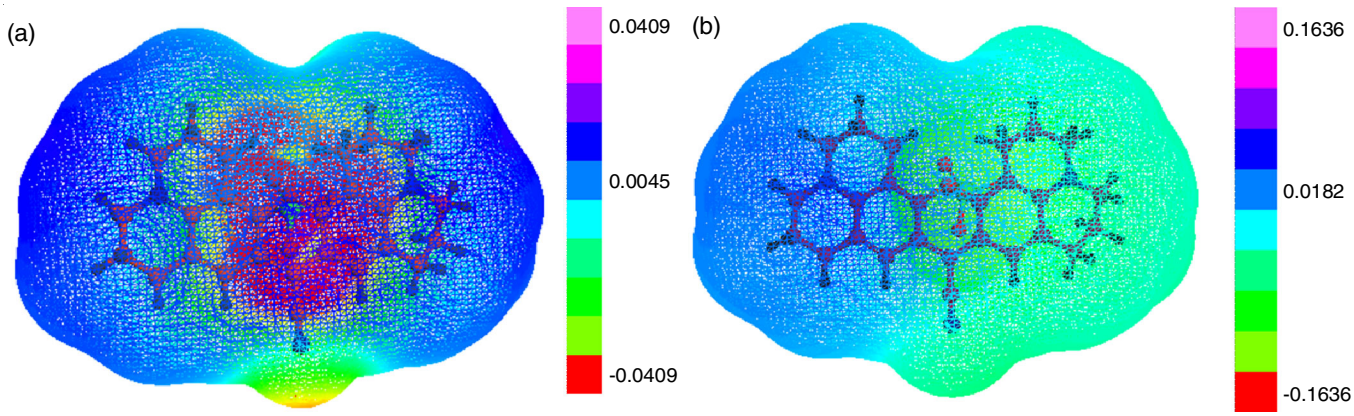

Fig. 9. MEP for Rh-800 (a) in vacuum (b) in ethanol

mation to molecular system due to atomic charges, electronic structure, acidity-basicity, molecular polarizability, dipole moment role and numerous characteristics of molecular system [57,58]. Atomic charges of each and every atom of Qu-390 and Rh-800 had been examined in vacuum and ethanol solvent to yield knowledge about electrical dipole moment originating from non-uniform dissemination of charges. Mullikan atomic charge dissemination both in vacuum and ethanol for Qu-390 and Rh-800 are tabulated in Tables 9 and 10. The improved pattern of Mulliken atomic charges has been graphically represented in Fig. 10. For Qu-390 in vacuum with atom number (C3, C4, C6, C9, C12, C14, C15) carbon atoms (N1, N7, N13) nitrogen atoms, (O11, O16) oxygen atoms exhibit negative charge (electron donor) through (C2, C5, C8, C10, C17) carbon atoms and all hydrogen atoms exhibits positive charge (electron acceptor). In ethanol solvent, a decrease in atomic charge of every atom of carbon, oxygen, nitrogen atoms occurred mostly, except slight increase in atomic charge of (C4, C6, C12, C15) carbon atoms [59]. There is a drastic decrease of atomic charge of (N13) nitrogen atom and slight increase of positive charge of most hydrogen atoms. For Rh-800 in vacuum with atom number (C2, C3, C7, C8, C11, C12, C13, C17, C18, C23, C27) carbon atoms, all oxygen and nitrogen atoms are negatively charged (electron donor) and every hydrogen atoms exhibits positive charge (electron acceptor). In ethanol solvent, a decrease

TABLE-9
MULLIKEN ATOMIC CHARGES FOR
Qu-390 in VACUUM AND ETHANOL

Atoms	Vacuum	Ethanol	Atoms	Vacuum	Ethanol
1 N	-0.5262	-0.4652	17 C	0.0097	0.0097
2 C	0.3836	0.2850	18 H	0.1367	0.1186
3 C	-0.0588	-0.0365	19 H	0.1161	0.1114
4 C	-0.0168	-0.0362	20 H	0.0583	0.0580
5 C	0.3075	0.2569	21 H	0.0876	0.0838
6 C	-0.0175	-0.0364	22 H	0.0592	0.0599
7 N	-0.3243	-0.3030	23 H	0.0592	0.0599
8 C	0.4798	0.2735	24 H	0.0845	0.0837
9 C	-0.1571	-0.0107	25 H	0.0888	0.1021
10 C	0.2485	0.0602	26 H	0.0888	0.1021
11 O	-0.7567	-0.7477	27 H	0.0651	0.0581
12 C	-0.0110	-0.0215	28 H	0.0777	0.0860
13 N	-0.3287	-0.0776	29H	0.0777	0.0860
14 C	-0.0506	-0.0328	30 H	0.0663	0.0662
15 C	-0.0131	-0.0176	31 H	0.0799	0.0809
16 O	-0.3754	-0.3377	32 H	0.0799	0.0809

in atomic charge of every atom is observed. For (C28) carbon atom in vacuum is positive charge (electron acceptor) whereas in ethanol it's negatively charged (electron donor). Every hydrogen atoms exhibits positive charge (electron acceptor) [60]. The charge dissemination either in vacuum and ethanol solvent indicates that there occurs substantial polar character,

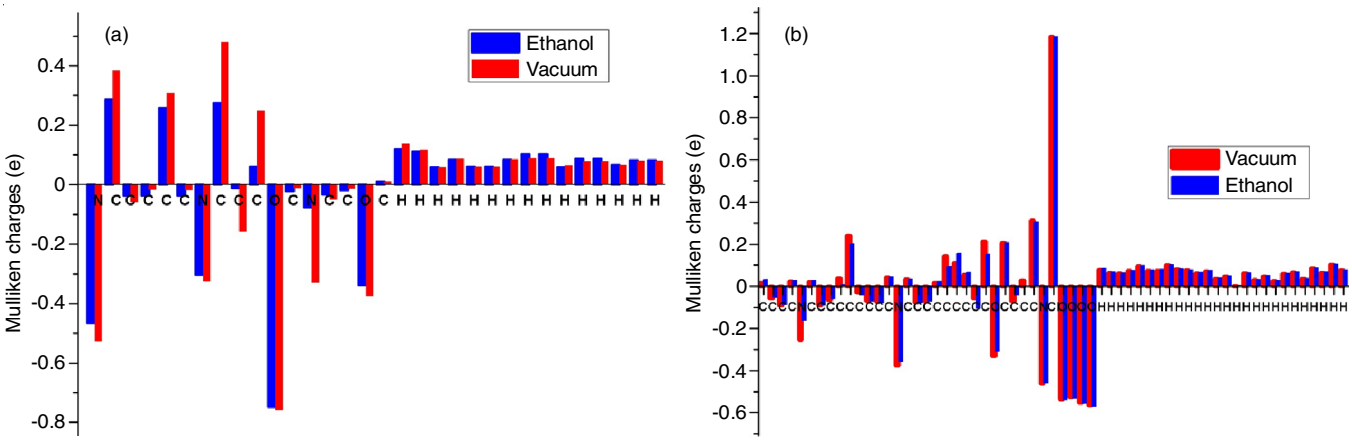

Fig. 10. Mulliken atomic charge distributions for (a) Qu-390 (b) Rh-800

directive from C-8 (Q = 0.4798) to O-11(Q = -0.7567) atom for Qu-390 and Cl-31 (charge value = 1.1848) chlorine atom to O-35 (charge value = -0.5663). Such a charge shift is attributed to the discrepancy between ground and first excited dipole moment states. Only positive values of hydrogen atoms imply the charge shifts from H-atom to other atoms.

Conclusion

The electronic absorption and fluorescence spectra of Qu-390 and Rh-800 have been resolved in various solvents having totally distinct solvatochromic constants. The absorption and fluorescence spectrum of the dyes display a major dependency of non-specific and specific solvent-solute interactions. Multi-parameter linear regression studies on absorption spectrum bestowed different coefficients correlation values, which suggests that observational articulations utilized are advantageous for assessing solvents consequences on the electronic absorption spectrum of laser dyes. A noticeable shift within the fluorescence emission spectrum of these laser dyes was seen within the solvents. The spectral shift was connected with solvent polarity (ε, n) and which is an indicator of rise in the electric-dipole moment on emission. Also the electrochemical and optical properties is examined by using TD-DFT computational techniques. Lowering of HOMO-LUMO band energy gap for Rh-800 is less than Qu-390, hence Rh-800 is considered as high reactive and soft than Qu-390, which endorses bioactive characteristics of laser dye. A charge transfer between atoms is attributed to the discrepancy between ground and first excited dipole moment states. Molecular electrostatic potential offers the visual illustration of electrophilic and nucleophilic reactivity sites. Established on above records, it is inferred that the laser dyes might be a very appealing entity for deceitful non-linear optical tools.

CONFLICT OF INTEREST

The authors declare that there is no conflict of interests regarding the publication of this article.

REFERENCES

1. C.M. da Silva, D.L. da Silva, L.V. Modolo, R.B. Alves, M.A. de Resende, C.V.B. Martins and A. de Fátima, *J. Adv. Res.*, **2**, 1 (2011); https://doi.org/10.1016/j.jare.2010.05.004.
2. J. Catalan, *J. Phys. Chem. B*, **113**, 5951 (2009); https://doi.org/10.1021/jp8095727.
3. M.J. Kamlet and R.W. Taft, *J. Am. Chem. Soc.*, **98**, 377 (1976); https://doi.org/10.1021/ja00418a009.
4. C. Gasbarri and G. Angelini, *J. Mol. Liq.*, **229**, 185 (2017); https://doi.org/10.1016/j.molliq.2016.12.033.
5. G.T. Tigineh and L.-K. Liu, *J. Photochem. Photobiol. Chem.*, **338**, 161 (2017); https://doi.org/10.1016/j.jphotochem.2017.02.001.
6. C.G. Renuka, K. Shivashankar, P. Boregowda, S.S. Bellad, M.V. Muregendrappa and Y.F. Nadaf, *J. Solution Chem.*, **46**, 1535 (2017); https://doi.org/10.1007/s10953-017-0661-4.
7. M. Homocianu and A. Airinei, *J. Fluoresc.*, **26**, 1617 (2016); https://doi.org/10.1007/s10895-016-1848-6.
8. M.S. Masoud, E.A. Khalil, S.A. Abou El-Enein and H.M. Kamel, *Eur. J. Chem.*, **2**, 420 (2011).
9. M.M. Miotke and M. Jozefowicz, *J. Mol. Liq.*, **230**, 129 (2017); https://doi.org/10.1016/j.molliq.2016.12.094.
10. D. Li, C. Li and Y. Liu, *J. Mol. Liq.*, **218**, 670 (2016); https://doi.org/10.1016/j.molliq.2016.02.084.
11. I.A.Z. Al-Ansari, *J. Fluoresc.*, **26**, 821 (2016); https://doi.org/10.1007/s10895-016-1770-y.
12. D. Dorohoi, *Spectrochim. Acta A Mol. Biomol. Spectrosc.*, **75**, 1030 (2010); https://doi.org/10.1016/j.saa.2009.12.046.
13. M.S. Mehata, A.K. Singh and R.K. Sinha, *J. Mol. Liq.*, **231**, 39 (2017); https://doi.org/10.1016/j.molliq.2017.01.091.
14. M. Pannipara, A.M. Asiri, K.A. Alamry, I.A. Salem and S.A. El-Daly, *J. Fluoresc.*, **25**, 103 (2015); https://doi.org/10.1007/s10895-014-1485-x.
15. C. Reichardt, Solvent and Solvent Effects in Organic Chemistry, Wiley, VCH, Verlach, GmbH&Co. KGaA: Weinheim, edn 3 (2004).
16. M.S. Masoud, A.E.H. Abdou and W.M. Ahmed, *J. Mol. Struct.*, **1095**, 135 (2015); https://doi.org/10.1016/j.molstruc.2015.04.007.
17. M.S. Masoud, S.S. Hagagg, A.E. Ali and N.M. Nasr, *Spectrochim. Acta A Mol. Biomol. Spectrosc.*, **94**, 256 (2012); https://doi.org/10.1016/j.saa.2012.03.037.
18. M.S. Masoud, A.M. Ramadan, A.A. Soayed and S.M.S. Ammar, *J. Iran. Chem. Soc.*, **13**, 931 (2016); https://doi.org/10.1007/s13738-016-0809-y.
19. I. Sidir, Y. Gülseven Sidir, H. Berber and E. Tasal, *J. Mol. Liq.*, **178**, 127 (2013); https://doi.org/10.1016/j.molliq.2012.11.011.
20. M.S. Masoud, A.E. Ali, D.A. Ghareeb and N.M. Nasr, *J. Mol. Liq.*, **224**, 914 (2016); https://doi.org/10.1016/j.molliq.2016.09.116.
21. M.S. Masoud, A.M. Hindawy, A.A. Soayed and M.Y. Abd El-Kaway, *Fluid Phase Equilib.*, **312**, 37 (2011); https://doi.org/10.1016/j.fluid.2011.08.028.
22. A. Tan, E. Bozkurt and Y. Kara, *J. Fluoresc.*, **27**, 981 (2017); https://doi.org/10.1007/s10895-017-2033-2.
23. R. Kumari, A. Varghese, L. George and Y.N. Sudhakar, *RSC Adv.*, **7**, 24204 (2017); https://doi.org/10.1039/C7RA01705G.

24. C. Zhai, B. Hou, P. Peng, P. Zhang, L. Li and X. Chen, *J. Mol. Liq.*, **249**, 9 (2018); https://doi.org/10.1016/j.molliq.2017.11.034.
25. M.S. Masoud, M.A. Shaker, A.E. Ali and G.S. Elasal, *Spectrochim. Acta A Mol. Biomol. Spectrosc.*, **79**, 538 (2011); https://doi.org/10.1016/j.saa.2011.03.029.
26. M.S. Masoud, H.M. Kamel and A.E. Ali, *Spectrochim. Acta A Mol. Biomol. Spectrosc.*, **137**, 1417 (2015); https://doi.org/10.1016/j.saa.2014.09.026.
27. B. Jedrzejewska, P. Krawczyk and M. Józefowicz, *Spectrochim. Acta A Mol. Biomol. Spectrosc.*, **171**, 258 (2017); https://doi.org/10.1016/j.saa.2016.08.006.
28. Y.G. Sidir and I. Sidir, *Spectrochim. Acta A Mol. Biomol. Spectrosc.*, **102**, 286 (2012); https://doi.org/10.1016/j.saa.2012.10.018.
29. R. Kumari, A. Varghese and L. George, *J. Lumin.*, **179**, 518 (2016); https://doi.org/10.1016/j.jlumin.2016.07.022.
30. M.A. Hussein, O.I. Osman, A.M. Asiri, H.D. Rozman and S.A. El-Daly, *J. Fluoresc.*, **27**, 1129 (2017); https://doi.org/10.1007/s10895-017-2048-8.
31. M. Panigrahi, S. Patel and B.K. Mishra, *J. Mol. Liq.*, **177**, 335 (2013); https://doi.org/10.1016/j.molliq.2012.09.021.
32. H. Qian, T. Tao, Y. Feng, Y. Wang and W.J. Huang, *J. Mol. Struct.*, **1123**, 305 (2016); https://doi.org/10.1016/j.molstruc.2016.06.042.
33. T. Tao, Y. Wang, Y. Dai, H. Qian and W. Huang, *Spectrochim. Acta A Mol. Biomol. Spectrosc.*, **136**, 1001 (2015); https://doi.org/10.1016/j.saa.2014.09.123.
34. M. Avadanei, V. Cozan and O. Avadanei, *J. Mol. Liq.*, **227**, 76 (2017); https://doi.org/10.1016/j.molliq.2016.11.124.
35. M.W. Schmidt, K.K. Baldridge, J.A. Boatz, S.T. Elbert, M.S. Gordon, J.H. Jensen, S. Koseki, N. Matsunaga, K.A. Nguyen, S. Su, T.L. Windus, M. Dupuis and J.A. Montgomery, *J. Comput. Chem.*, **14**, 1347 (1993); https://doi.org/10.1002/jcc.540141112.
36. A.G. Al Sehemi, M. Pannipara, A. Kalam and A.M. Asiri, *J. Fluoresc.*, **26**, 1357 (2016); https://doi.org/10.1007/s10895-016-1823-2.
37. R.P. Tayade and N. Sekar, *J. Fluoresc.*, **27**, 167 (2017); https://doi.org/10.1007/s10895-016-1943-8.
38. J. Jayabharathi, V. Kalaiarasi, V. Thanikachalam and K. Jayamoorthy, *J. Fluoresc.*, **24**, 599 (2014); https://doi.org/10.1007/s10895-013-1334-3.
39. E.E. Porchelvi and S. Muthu, *Spectrochim. Acta A Mol. Biomol. Spectrosc.*, **134**, 453 (2015); https://doi.org/10.1016/j.saa.2014.06.018.
40. K. Chandrasekaran and R. Thilak Kumar, *Spectrochim. Acta A Mol. Biomol. Spectrosc.*, **150**, 974 (2015); https://doi.org/10.1016/j.saa.2015.06.018.
41. A. Suvitha, S. Periandy and P. Gayathri, *Spectrochim. Acta A Mol. Biomol. Spectrosc.*, **138**, 357 (2015); https://doi.org/10.1016/j.saa.2014.11.011.
42. S. Chand, F.A.M. Al-Omary, A.A. El-Emam, V.K. Shukla, O. Prasad and L. Sinha, *Spectrochim. Acta A Mol. Biomol. Spectrosc.*, **146**, 129 (2015); https://doi.org/10.1016/j.saa.2015.03.068.
43. S.M. Soliman, M. Hagar, F. Ibid and E.S.H. El Ashry, *Spectrochim. Acta A Mol. Biomol. Spectrosc.*, **145**, 270 (2015); https://doi.org/10.1016/j.saa.2015.01.061.
44. S.M. Soliman, J. Albering and M.A.M. Abu-Youssef, *Spectrochim. Acta A Mol. Biomol. Spectrosc.*, **136**, 1086 (2015); https://doi.org/10.1016/j.saa.2014.09.133.
45. N. Prabavathi, N. Senthil Nayaki and B. Venkatram Reddy, *Spectrochim. Acta A Mol. Biomol. Spectrosc.*, **136**, 1134 (2015); https://doi.org/10.1016/j.saa.2014.09.137.
46. V. Balachandran, G. Santhi, V. Karpagam, B. Revathi and M. Karabacak, *Spectrochim. Acta A Mol. Biomol. Spectrosc.*, **136**, 451 (2015); https://doi.org/10.1016/j.saa.2014.09.057.
47. A.M. Al-Soliemy, O.I. Osman, M.A. Hussein, A.M. Asiri and S.A. El-Daly, *J. Fluoresc.*, **26**, 1199 (2016); https://doi.org/10.1007/s10895-016-1802-7.
48. J. Jayabharathi, V. Thanikachalam, V. Kalaiarasi and K. Jayamoorthy, *J. Photochem. Photobiol. Chem.*, **275**, 114 (2014); https://doi.org/10.1016/j.jphotochem.2013.11.006.
49. M. Toy and H. Tanak, *Spectrochim. Acta A Mol. Biomol. Spectrosc.*, **152**, 530 (2016); https://doi.org/10.1016/j.saa.2014.11.003.
50. Y.G. Sidir and I. Sidir, *J. Mol. Liq.*, **211**, 591 (2015); https://doi.org/10.1016/j.molliq.2015.07.053.
51. I. Sidir and Y.G. Sidir, *Spectrochim. Acta A Mol. Biomol. Spectrosc.*, **135**, 560 (2015); https://doi.org/10.1016/j.saa.2014.07.049.
52. F. Naderi and A. Farajtabar, *J. Mol. Liq.*, **221**, 102 (2016); https://doi.org/10.1016/j.molliq.2016.05.071.
53. I. Sidir, Y.G. Sidir, H. Berber and F. Demiray, *J. Mol. Liq.*, **206**, 56 (2015); https://doi.org/10.1016/j.molliq.2015.01.056.
54. A.S. Choudhary and N. Sekar, *J. Fluoresc.*, **25**, 675 (2015); https://doi.org/10.1007/s10895-015-1553-x.
55. A.M. Asiri, S.A. Ahmed, S.A. El-Daly, M.A. Hussein, A.M. Al-Soliemy, O.I. Osman, M.R. Shaaban and I.I. Althagafi, *J. Fluoresc.*, **25**, 1303 (2015); https://doi.org/10.1007/s10895-015-1618-x.
56. A.M. Asiri, T.R. Sobahi, O.I. Osman and S.A. Khan, *J. Mol. Struct.*, **1128**, 636 (2017); https://doi.org/10.1016/j.molstruc.2016.08.081.
57. S.A. El-Daly and K.A. Alamry, *J. Fluoresc.*, **26**, 163 (2016); https://doi.org/10.1007/s10895-015-1698-7.
58. N. Nagarajan, G. Velmurugan, G. Prabhu, P. Venuvanalingam and R. Renganathan, *J. Lumin.*, **147**, 111 (2014); https://doi.org/10.1016/j.jlumin.2013.11.010.
59. N. Nagarajan, G. Velmurugan, P. Venuvanalingam and R. Renganathan, *J. Photochem. Photobiol. Chem.*, **284**, 36 (2014); https://doi.org/10.1016/j.jphotochem.2014.04.008.
60. A. Georgiev, A. Kostadinov, D. Ivanov, D. Dimov, S. Stoyanov, L. Nedelchev, D. Nazarova and D. Yancheva, *Spectrochim. Acta A Mol. Biomol. Spectrosc.*, **192**, 263 (2018); https://doi.org/10.1016/j.saa.2017.11.016.